A Transcriptomic Network Underlies Microstructural and Physiological Responses to Cadmium in *Populus* × *canescens*[1][C][W]

Jiali He[2], Hong Li[2], Jie Luo, Chaofeng Ma, Shaojun Li, Long Qu, Ying Gai, Xiangning Jiang, Dennis Janz, Andrea Polle, Melvin Tyree, and Zhi-Bin Luo*

College of Life Sciences and State Key Laboratory of Crop Stress Biology in Arid Areas (J.H., J.L., C.M., S.L., Z.-B.L.), Key Laboratory of Applied Entomology, College of Plant Protection (H.L.), and Key Laboratory of Environment and Ecology in Western China, Ministry of Education, College of Forestry (M.T., Z.-B.L.), Northwest A&F University, Yangling, Shaanxi 712100, China; National Engineering Laboratory of Tree Breeding, College of Life Sciences and Biotechnology, Beijing Forestry University, Beijing 100083, China (L.Q., Y.G., X.J.); and Büsgen Institute, Department of Forest Botany and Tree Physiology, Georg-August University, 37077 Göttingen, Germany (D.J., A.P.)

Bark tissue of *Populus* × *canescens* can hyperaccumulate cadmium, but microstructural, transcriptomic, and physiological response mechanisms are poorly understood. Histochemical assays, transmission electron microscopic observations, energy-dispersive x-ray microanalysis, and transcriptomic and physiological analyses have been performed to enhance our understanding of cadmium accumulation and detoxification in *P.* × *canescens*. Cadmium was allocated to the phloem of the bark, and subcellular cadmium compartmentalization occurred mainly in vacuoles of phloem cells. Transcripts involved in microstructural alteration, changes in nutrition and primary metabolism, and stimulation of stress responses showed significantly differential expression in the bark of *P.* × *canescens* exposed to cadmium. About 48% of the differentially regulated transcripts formed a coregulation network in which 43 hub genes played a central role both in cross talk among distinct biological processes and in coordinating the transcriptomic regulation in the bark of *P.* × *canescens* in response to cadmium. The cadmium transcriptome in the bark of *P.* × *canescens* was mirrored by physiological readouts. Cadmium accumulation led to decreased total nitrogen, phosphorus, and calcium and increased sulfur in the bark. Cadmium inhibited photosynthesis, resulting in decreased carbohydrate levels. Cadmium induced oxidative stress and antioxidants, including free proline, soluble phenolics, ascorbate, and thiol compounds. These results suggest that orchestrated microstructural, transcriptomic, and physiological regulation may sustain cadmium hyperaccumulation in *P.* × *canescens* bark and provide new insights into engineering woody plants for phytoremediation.

Cadmium is a nonessential and highly toxic element for plants. Cadmium in soil enters plants via transporters for essential elements (e.g. calcium, iron, and zinc) and is eventually taken up by the human body through the food chain. Cadmium accumulation in humans may cause prostate and lung cancers and bone fractures (Bertin and Averbeck, 2006; Nawrot et al., 2006). Thus, it is extremely important to remediate cadmium-polluted soils. Phytoremediation is an efficient and effective biotechnology to extract cadmium from soil via harvestable portions of plants (Kramer, 2010; Mendoza-Cózatl et al., 2011).

There are numerous consequences of cadmium toxicity in plants. Soil cadmium enters plants via apoplastic and/or symplastic pathways. The cadmium subsequently poisons tissues, causing changes in subcellular structures and altering physiological and molecular processes (Kramer, 2010; Mendoza-Cózatl et al., 2011). Cadmium can modify cell wall structure and degenerate cellular organelles such as chloroplasts and mitochondria (Van Belleghem et al., 2007). Ionic Cd (Cd^{2+}) may compete with nutrient cations (e.g. Ca^{2+}, Fe^{2+}, and Zn^{2+}) for transporters, often leading to decreases in these essential elements and to disruptions in the ionic homeostasis of plants (Rodríguez-Serrano et al., 2009). In particular, cadmium exposure may provoke iron deficiency in plants due to competition for iron transporters between Cd^{2+} and Fe^{2+}

[1] This work was supported by the Special Fund for Forest Science and Technology Research in the Public Interest (grant no. 201204210), the State Key Basic Research Development Program (grant no. 2012CB416902), the National Natural Science Foundation of China (grant nos. 31070539, 31100481, and 31270647), the Program for New Century Excellent Talents in University from the Ministry of Education of China (grant no. NCET–08–0468), and the German Science Foundation (grant no. INST 186/766–1 FUGG).

[2] These authors contributed equally to the article.

* Corresponding author; e-mail luozbbill@163.com.

The author responsible for distribution of materials integral to the findings presented in this article in accordance with the policy described in the Instructions for Authors (www.plantphysiol.org) is: Zhi-Bin Luo (luozbbill@163.com).

[C] Some figures in this article are displayed in color online but in black and white in the print edition.

[W] The online version of this article contains Web-only data.

www.plantphysiol.org/cgi/doi/10.1104/pp.113.215681

(Besson-Bard et al., 2009; Wu et al., 2012). Repression of photosynthesis is frequently observed in plants exposed to cadmium due to damage of the photosynthetic apparatus (Cunha et al., 2008). This can alter carbohydrate concentrations throughout all plant tissues (He et al., 2011). Cadmium in plants can indirectly induce hydrogen peroxide (H_2O_2) and superoxide ($O_2^{\bullet-}$), giving rise to an oxidative burst (Rodríguez-Serrano et al., 2009). Moreover, cadmium exposure can bring about differential expression of genes involved both in cadmium transport and in scavenging reactive oxygen species (ROS) in plants (Küpper and Kochian, 2010).

Plants have evolved several strategies for cadmium detoxification. First, the apoplast acts as a barrier for cadmium entry because Cd^{2+} binds to polyuronic acids and pectin in plant cell walls (Conn and Gilliham, 2010) and stimulates increased lignification (Schützendübel et al., 2001; Elobeid et al., 2012). Second, cadmium entry into the symplast can be detoxified by cadmium chelates in cytosol and sequestration in vacuoles. Ionic cadmium in cytosol can bind to reduced glutathione (GSH) and phytochelatins (PCs), forming cadmium-ligands that are subsequently transported to vacuoles, where cadmium can be sequestered (Conn and Gilliham, 2010; Park et al., 2012). Finally, cadmium stress activates several biochemical defenses, such as antioxidative enzymes and GSH synthesis, thus leading to reprogramming of the root or leaf transcriptome (Herbette et al., 2006; Mendoza-Cózatl et al., 2008; Rodríguez-Serrano et al., 2009; Xu et al., 2012).

The above-mentioned processes of cadmium toxicity and detoxification have been explored mostly in herbaceous plants such as Arabidopsis (*Arabidopsis thaliana*), *Arabidopsis halleri*, and *Thlaspi caerulescens* (Kramer, 2010; Mendoza-Cózatl et al., 2011). However, the limited biomass of herbaceous plants constrains their application for phytoremediation on a large scale. Poplars (*Populus* spp.) have been proposed for phytoremediation because of their rapid growth, deep root system, and relatively high cadmium accumulation in some genotypes (Merkle, 2006; He et al., 2013). The cadmium entering roots can be transported to leaves along with the transpiration stream and can be further translocated to the bark, where high accumulation occurs in *Populus* × *canescens* grown in hydroponics (He et al., 2011).

Bark contains phloem tissue, which plays a crucial role in delivering nutrients to sink tissues (e.g. new shoots and roots), thereby contributing to internal cadmium allocation. Thus, it is essential to understand cadmium toxicity and detoxification in the bark of *P.* × *canescens* to restrict recycling of cadmium to roots, particularly in terms of using *P.* × *canescens* to remediate cadmium-polluted soils. Although responses of poplars to cadmium stress have been investigated at the proteomic and physiological levels (Schützendübel et al., 2002; Kieffer et al., 2008, 2009a, 2009b; Durand et al., 2010; He et al., 2011), the microstructural, transcriptomic, and physiological mechanisms underlying cadmium toxicity and detoxification remain unknown in the bark of poplars.

To elucidate cadmium distribution and transcriptomic and physiological regulation mechanisms in the bark, hybrid poplars (*P.* × *canescens*) were exposed to 0 or 200 μM $CdSO_4$. These cadmium concentrations were within the range (0–500 μM Cd^{2+}) used in previous studies (Ager et al., 2003; Wójcik and Tukiendorf, 2004; Mendoza-Cózatl et al., 2011). The objective of this paper is to address the following questions. (1) Where is cadmium localized at the subcellular level, and is the ultrastructure of the bark altered in response to cadmium exposure? (2) Are these alterations associated with transcriptomic reprogramming? (3) Do these changes lead to modifications of physiological processes in the bark after cadmium exposure? The bark tissue is the focus of this study, but root and leaf tissues have been included in the microstructural and physiological analyses because of the interconnection of cadmium transport among these tissues. A study addressing these questions will not only help us to better understand the microstructural, transcriptomic, and physiological regulation mechanisms of woody plants in response to cadmium exposure, but also provide new insights into engineering woody plants for phytoremediation.

RESULTS

Cadmium Results in Granular Deposition and Causes Microstructural Changes

Plants of *P.* × *canescens* grown in sand cultures were exposed to a cadmium concentration, which reduced but did not abolish growth (Supplemental Table S1). Under these conditions, the typical cadmium distribution pattern was observed, with higher concentrations in roots and lower concentrations in leaves and bark (Fig. 1). Still, cadmium concentrations in all analyzed tissues were well above the threshold of 100 μg g^{-1} dry weight commonly defined for hyperaccumulation

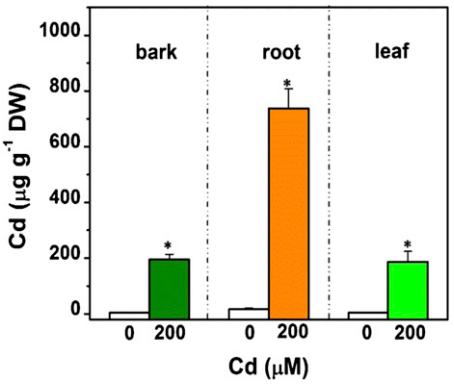

Figure 1. Cadmium concentrations in the bark, root, and leaf tissues of *P.* × *canescens* exposed to 0 (blank bars) or 200 μM (filled bars) $CdSO_4$ for 20 d. Bars indicate means ± SE (n = 6). Asterisks on the bars for the same tissue indicate significant differences between treatments. [See online article for color version of this figure.]

(Milner and Kochian, 2008). To investigate the cellular localization of cadmium in the bark compared with other tissues, we conducted histochemical staining for cadmium (Fig. 2). In stem cross sections, strong cadmium-dithizone staining was observed in the phloem, with formation of distinct granules (Fig. 2B). Notably, such granules were also observed on the surface (Fig. 2D) of fine roots and in the apoplast of root cortical cells (Fig. 2F). In leaves, cadmium-dithizone staining was observed mainly in leaf veins (Fig. 2H), in intercellular spaces of mesophyll cells near veins (Fig. 2H), in petioles, and in leaf trichomes (Supplemental Fig. S1). This suggests a preferential accumulation of cadmium along the transport path.

To corroborate cadmium accumulation in the granules, we studied the subcellular structures at higher magnification with transmission electron microscopy (TEM) and analyzed the elemental composition of the granular deposits by energy-dispersive x-ray (EDX) microanalysis (Figs. 3 and 4; Supplemental Figs. S2 and S3). Electron dense granules in vacuoles of phloem cells were observed in the bark of cadmium-exposed *P.* × *canescens*, whereas these granules were absent in controls (Fig. 3, A and B). EDX analysis of these granules in vacuoles of the phloem cells revealed strong accumulation of cadmium (Fig. 4A; Supplemental Fig. S2). These electron dense granules also contained sulfur and other elements such as aluminum and copper (Supplemental Fig. S2). Among these elements, a significant correlation was observed between cadmium and sulfur (Fig. 4B), indicating that cadmium may chelate with sulfur-containing ligands in *P.* × *canescens*. Cadmium accumulation in electron-dense granules was also detected in the vacuoles of root and mesophyll cells (Fig. 4A; for transmission electron microscopic micrographs, see Supplemental Fig. S3).

Microscopic analysis of the phloem also revealed that cadmium exposure altered the chloroplast structure (i.e. chloroplast grana were distorted in companion cells; Fig. 3, C–F). Furthermore, much fewer starch grains per cell were observed in cadmium-exposed plants (4.3 ± 0.1) than in control plants (13.3 ± 0.2, $P < 0.0001$; Fig. 3, C–F). Moreover, compared with control *P.* × *canescens*, mitochondria in companion

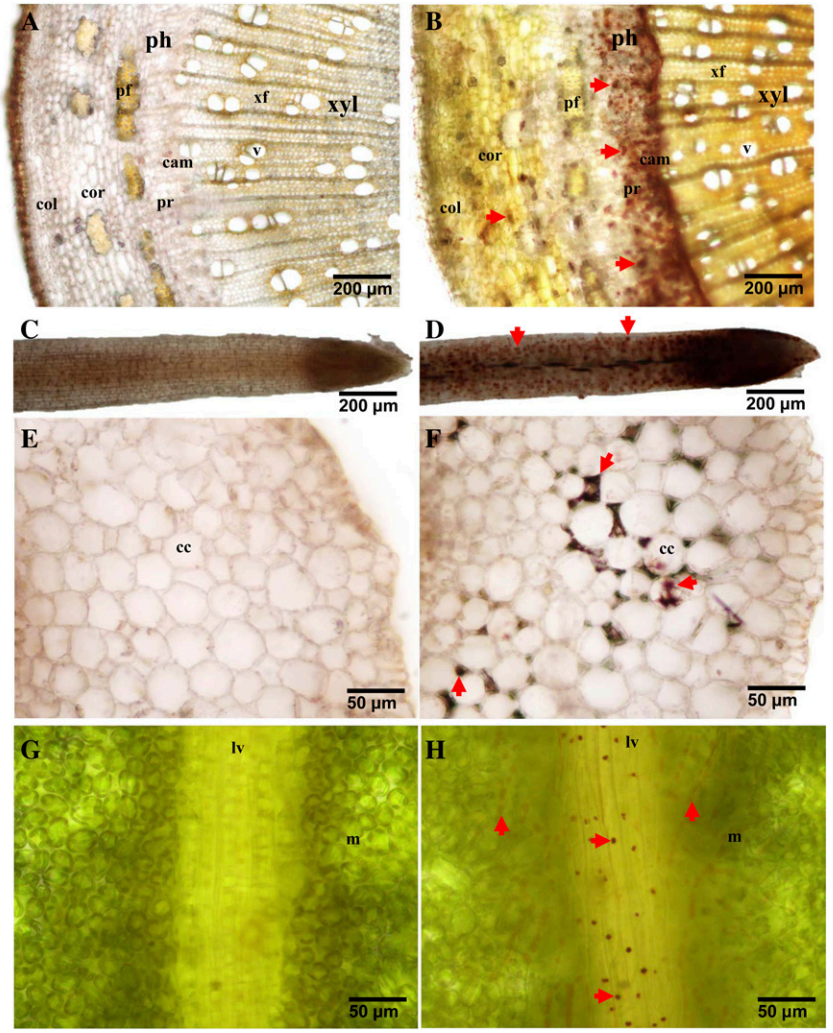

Figure 2. Cadmium localization in the bark (A and B), root (C–F), and leaf tissues (G and H) of *P.* × *canescens* exposed to 0 (A, C, E, and G) or 200 μM (B, D, F, and H) $CdSO_4$ for 20 d. Arrows point to precipitates of cadmium-dithizone. B, Cadmium-dithizone precipitates in the bark. D, Cadmium-dithizone precipitates in epidermal cells of fine roots. F, Cadmium-dithizone precipitates in intercellular spaces, cell walls, and cytoplasm of cortical cells. H, Cadmium-dithizone precipitates in leaf veins and in intercellular spaces of mesophyll cells. col, Collenchyma; cor, cortex; pf, phloem fiber; pr, phloem ray; ph, phloem; cam, cambium; v, vessel; xf, xylem fiber; xyl, xylem; cc, cortical cells; lv, leaf vein; m, mesophyll cells. [See online article for color version of this figure.]

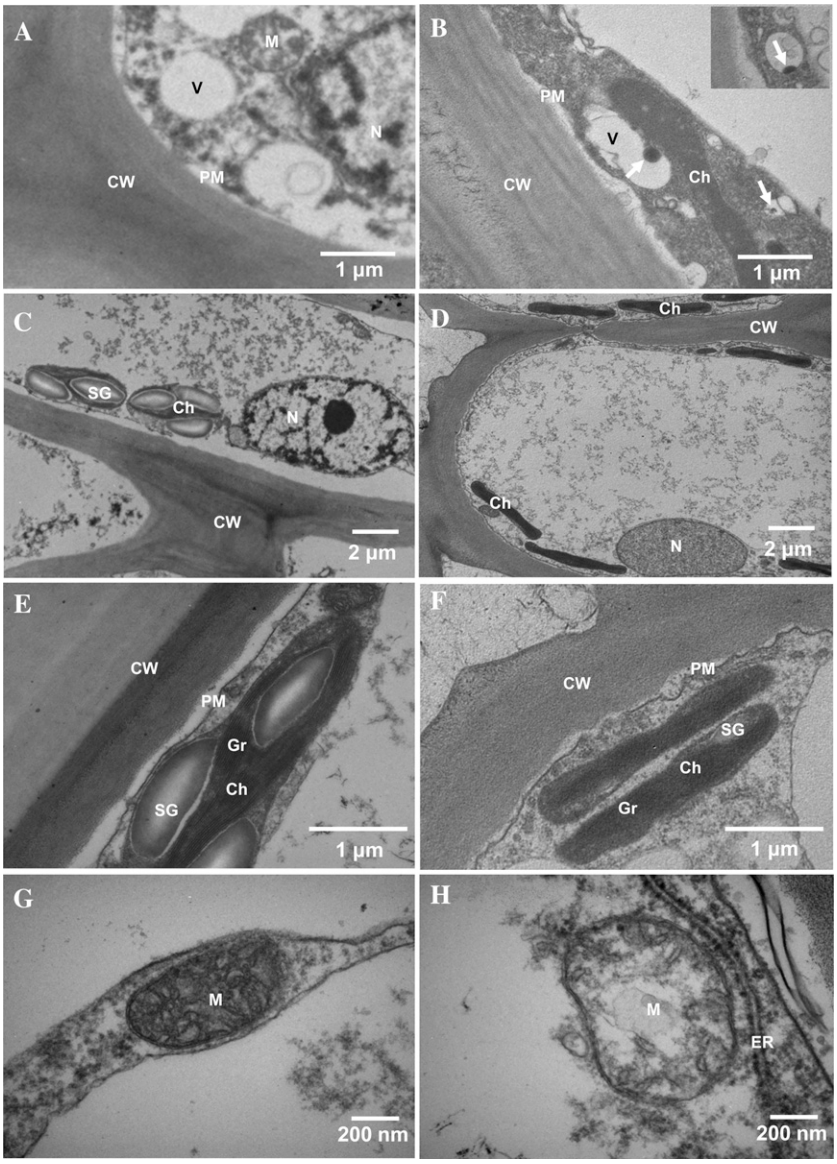

Figure 3. Transmission electron microscopic micrographs of granular deposits in vacuoles of phloem cells (A and B) and companion cells (C–H) in the bark of *P.* × *canescens* exposed to 0 (A, C, E, and G) or 200 μM (B, D, F, and H) $CdSO_4$ for 20 d. The insert in B highlights a granular deposit in a vacuole. Arrows point to cadmium deposits. Cadmium concentrations in granular deposits are shown in Figure 4A. The EDX spectra of vacuoles (A) and granular deposits in vacuoles (B) are shown in Supplemental Figure S2. CW, Cell wall; PM, plasma membrane; N, nucleus; V, vacuole; Ch, chloroplast; Gr, granum; SG, starch grain; M, mitochondrion; ER, endoplasmic reticulum.

cells of the phloem appeared swollen in cadmium-treated plants, and the cristae displayed an irregular shape (Fig. 3, G and H). These results suggest that cadmium toxicity may cause partial disorganization of chloroplasts and mitochondria via membrane degradation of subcellular structures in companion cells of *P.* × *canescens*.

A Transcriptomic Coexpression Network Responds to Cadmium in the Bark

To find out how cadmium accumulation altered molecular functioning in bark tissue, we conducted genome-wide transcriptional analyses of *P.* × *canescens* bark using Affymetrix poplar genome arrays. After cadmium exposure, 505 genes showed significant increases in transcript abundance in *P.* × *canescens* bark, whereas 366 genes showed significant decreases (Supplemental Table S2). Among these differentially regulated transcripts, 302 up-regulated and 223 down-regulated transcripts were identified that had corresponding annotations for homologs in Arabidopsis (Supplemental Table S2). To further categorize the functions of cadmium-responsive poplar genes, all unique Arabidopsis gene identifiers (AGIs) were selected. The 484 genes that were identified were further analyzed in MapMan (Figs. 5 and 6; Supplemental Table S3). An overview of functional categories revealed that most of the cadmium-responsive genes were involved in the regulation and processing of RNA and proteins, as well as in signaling and stress (Fig. 5). A closer look at the categories revealed that 20 of the genes in the protein category belonged to the 26S proteasome complex, which mediates ubiquitin-dependent protein degradation (Supplemental Table S3). In the

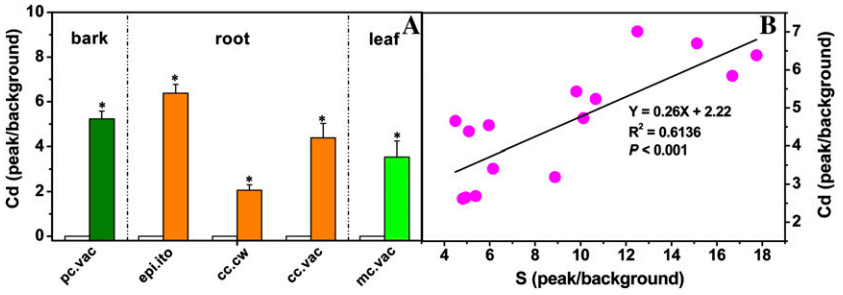

Figure 4. EDX analysis determined cadmium concentrations (A) and the correlation between cadmium and sulfur (B) in granules of different cell compartments of *P.* × *canescens* exposed to 0 (blank bars) or 200 μM (filled bars) $CdSO_4$ for 20 d. Bars indicate means ± SE (n = 3). Asterisks on bars for the same cell compartment indicate significant differences between treatments. The data for correlation analysis were based on cadmium and sulfur concentrations in granules of all examined subcellular compartments. Transmission electron microscopic micrographs of cadmium-deposited granules in subcellular compartments of roots and leaves are shown in Supplemental Figure S3. pc.vac, Vacuoles of phloem cells; epi.ito, inside tonoplast of epidermal cells; cc.cw, cell walls of cortical cells; cc.vac, vacuoles of cortical cells; mc.vac, vacuoles of mesophyll cells. [See online article for color version of this figure.]

RNA regulation category, several transcription factors involved in biotic stress, such as WRKY70/53, MYB94, ABI5, and AP2, were activated (Fig. 6A; Supplemental Table S3). In the signaling category, genes involved in biotic stress signaling were activated. This included, for example, calmodulin-binding transcription activator and Leu-rich repeat protein kinase family protein (Fig. 6A; Supplemental Table S3). In the stress category, a few genes encoding pathogenesis-related (PR)-proteins, as well as genes implicated in cell wall metabolism such as glycosyl hydrolase9A4 and arabinogalactan protein6, were highly overexpressed (Fig. 6A; Supplemental Table S3). These data suggest that cadmium induced responses similar to those found after wounding and that these responses may have also invoked activation of cell wall metabolism. In addition, a number of genes involved in primary and secondary metabolisms were also significantly up-regulated (Fig. 6B). Overall, these findings suggest that cadmium induces a tightly regulated gene network for detoxification and metabolic reprogramming.

To corroborate this idea, coexpression analysis was conducted. Genes that cooperate in a shared function, for example, in response to abiotic and biotic stressors, are often expressed simultaneously (Wei et al., 2006). By investigating how transcriptomic patterns vary in concert across hundreds of microarray experiments, new insights may be gained about the roles of coordinated gene networks in plants (Wei et al., 2006; Ficklin and Feltus, 2011; Osorio et al., 2012). To check whether the differentially expressed genes were co-regulated in the bark of cadmium-treated *P.* × *canescens*, genes with unique AGIs (Supplemental Table S3) were used as query genes in the CressExpress database version 2.0 (http://cressexpress.org/index.jsp), which has analyzed correlations between genes on 486 arrays across various experimental conditions (Wei et al., 2006). Out of 484 query genes, 234 genes (approximately 48%) formed a cadmium-responsive coexpression network (Fig. 7A; Supplemental Table S3). In this cadmium-responsive network, 234 genes were directly connected with each other via 1,254 edges, suggesting that the coexpressed genes are most likely coregulated.

Forty-three of these coexpressed genes were strongly interconnected, with each gene having more than 20 edges (Fig. 7B). These genes were therefore defined as hub genes. The hub genes were directly connected with each other via 308 edges, forming a highly interconnected subnetwork (Fig. 7B; Supplemental Table S3). Highly connected hub genes have displayed a marked enrichment for cross talk among essentially biological processes (Heyndrickx and Vandepoele, 2012). Consistently,

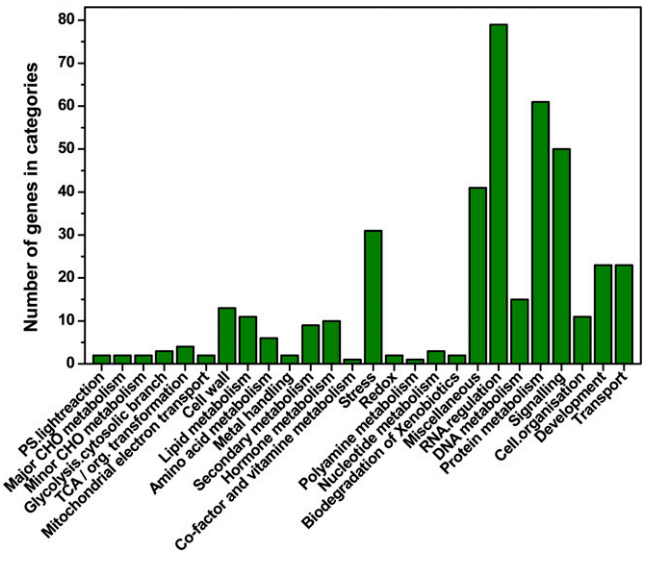

Figure 5. Number of genes assigned to each category by MapMan analysis. Detailed information for each category is presented in Supplemental Table S3. [See online article for color version of this figure.]

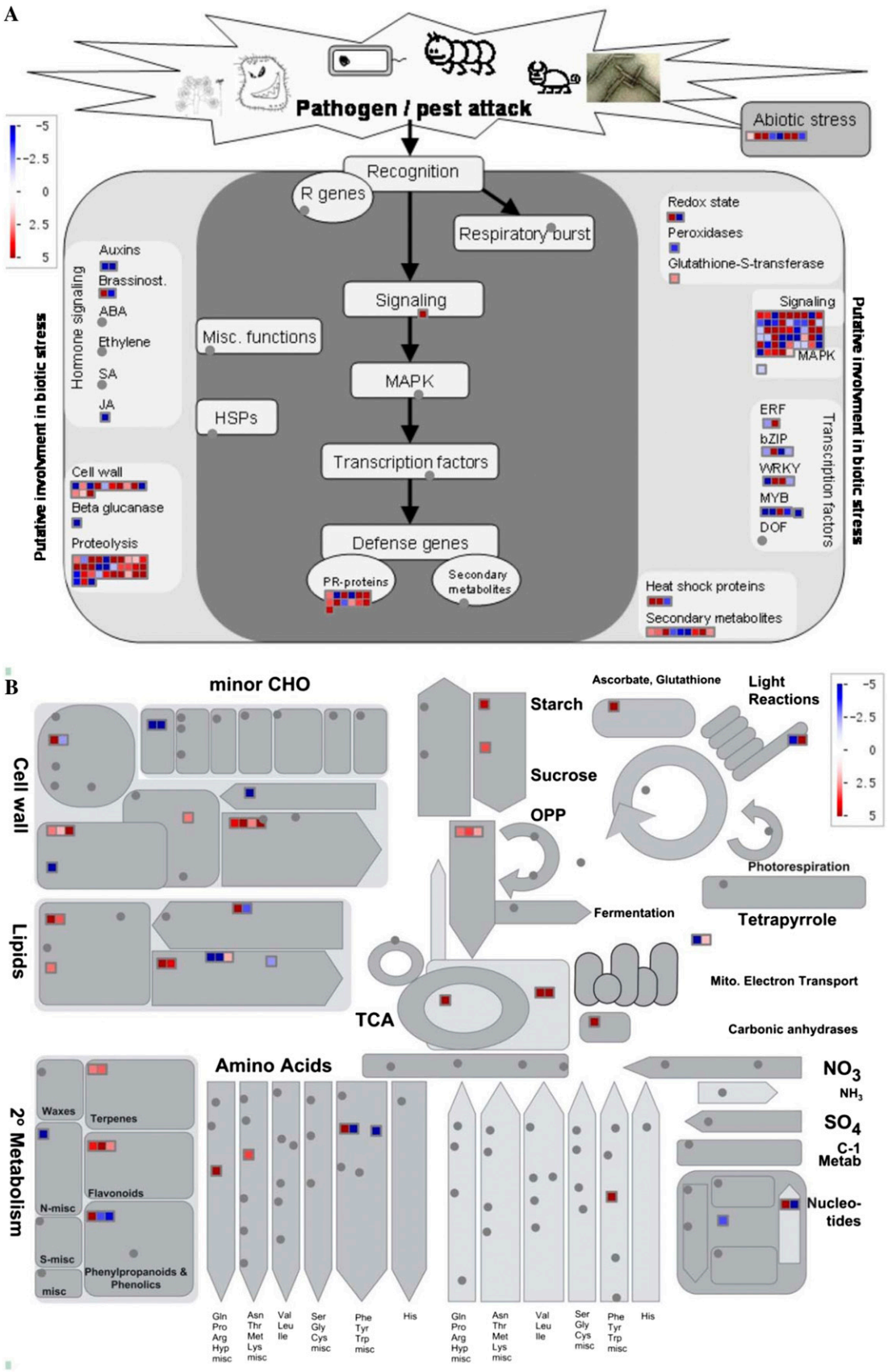

Figure 6. Transcripts involved in stress (A) and metabolism (B) assigned by MapMan in the bark of *P.* × *canescens* exposed to 0 or 200 μM $CdSO_4$ for 20 d. Positive fold change values (red) indicate up-regulation, whereas negative fold change values (blue)

10 out of 43 hub genes (approximately 23%) were in the signaling category when testing the functional assignments of the genes in MapMan (Supplemental Table S3). For instance, a putative wall-associated kinase, a GDP dissociation inhibitor family protein/Rab GTPase activator family protein, and a chloroplast sensor kinase were among these 10 hub genes involved in signaling (Fig. 7B; Supplemental Table S3). This suggests that coordinated cadmium signaling can take place across different subcellular compartments. Analysis of Gene Ontology (GO) term enrichment revealed that the hub genes were significantly enriched in processes related to transport, energy metabolism, photosynthesis, and isopentenyl diphosphate biosynthesis (Fig. 7C; redundant GO terms not shown). Isopentenyl diphosphate is the precursor for isoprenoids, which are essential building blocks for photosynthetic pigments, redox factors, hormones, feeding deterrents, and phytoalexins (Davies, 2010).

Analysis of GO term enrichment indicated 85 GO terms of all cadmium responsive genes and even 120 GO terms of the coexpressed genes for biological processes, molecular functions, and cellular compartments in which genes were strongly enriched (Supplemental Table S4). This finding suggests that coexpression analysis removed functionally less interconnected genes. For the coexpressed genes, some highly enriched, functionally different biological processes were biotic stimulus, cell tip growth, negative regulation of defense response, cell death, plant-type hypersensitive response, salicylic-mediated signaling pathway, protein targeting to membrane, developmental cell growth, plant-type cell wall organization or biogenesis, and protein phosphorylation (Supplemental Table S4). More than one-half of the coexpressed genes belonged to the primary metabolic process category (GO:0044238; Supplemental Table S4).

Overall, these results indicate that the response to cadmium involves strongly interlinked signaling and transcriptional regulation events, which may trigger transport processes for detoxification in vacuoles and cell walls, activate biochemical defense reactions, and influence subcellular microstructures.

The Cadmium Transcriptome Is Linked with Bark-Specific Physiological Readouts

To identify key metabolic processes that were affected by cadmium, we investigated the internal nutrient status, carbohydrate metabolism, oxidative stress, and antioxidants in *P.* × *canescens* (Supplemental Figs. S4–S6; Supplemental Tables S5 and S6). Moreover, to find out if the response of bark tissue to cadmium was similar to that of root and leaf tissues, we compared the response patterns of nutrients, carbohydrates, and oxidants and antioxidants using principal component analysis (PCA; Fig. 8; Supplemental Table S7). The first component, principal component 1 (PC1), of PCA for nutrient status clearly separated bark, root, and leaf tissues, accounting for 60% of the variation (Fig. 8A). The second component, principal component 2 (PC2), which accounted for 20% of the variation, separated the cadmium effect from the controls in root and leaf tissues; however, the separation was not as pronounced in bark tissue (Fig. 8A). This observation indicates that bark nutrient status was much less influenced by cadmium than other tissues were. The one exception was phosphorus concentration, which strongly declined by 27% (Supplemental Table S5). Compared with the control, the bark of cadmium-exposed *P.* × *canescens* had lower total nitrogen, phosphorus, and calcium concentrations, but higher sulfur concentrations. (Supplemental Table S5). This is in line with the idea that differentially expressed genes are involved in nutrient homeostasis, such as nitrate transporters (NRT2;4 and NRT1;7), phosphate transporters (PHT1;4 and PHT3;3), and a calcium-binding elongation factor-hand family protein (Supplemental Table S3).

The PCA of sugars and sugar alcohols in the bark, root, and leaf tissues shows that PC1 also separated the three tissues and accounted for 69% of the variation (Fig. 8B). The PC2 displayed a clear cadmium effect in all three tissue types, and Suc was the most important contributor to PC2 (Fig. 8B; Supplemental Table S7). The depletion of carbohydrates in the bark of cadmium-exposed *P.* × *canescens* was corroborated by a reduction in the number of starch grains (Fig. 3) and the overexpression of two genes involved in Suc and starch degradation (i.e. a chloroplast-targeted alkaline/neutral invertase and a chloroplastidic phosphoglucan, water dikinase; Fig. 6B; Supplemental Table S6). Stimulation of cell wall metabolism and activation of energy-requiring defenses may have contributed to the consumption of carbohydrates. This can also be inferred from increased transcript levels of enzymes involved in anapleurotic reactions, lipid degradation, and the citrate cycle. Furthermore, inhibited CO_2 assimilation in cadmium-exposed poplars (Supplemental Table S1) may have resulted in lower Suc transport from leaves to sink tissues. In agreement with decreased transcripts involved in inositol and mannitol metabolism, such as galactinol synthase1 and raffinose synthase5 (Fig. 6B; Supplemental Table S3), those sugar alcohols were reduced in the bark of cadmium-exposed *P.* × *canescens* (Supplemental Table S6).

PCA of oxidants and antioxidants in the bark, root, and leaf tissues shows that PC1 separated the tissues. PC2 separated the cadmium effect in bark and leaf

Figure 6. (*Continued.*)
denote down-regulation. Color saturates at 5-fold change. Each square represents a differentially expressed transcript. [See online article for color version of this figure.]

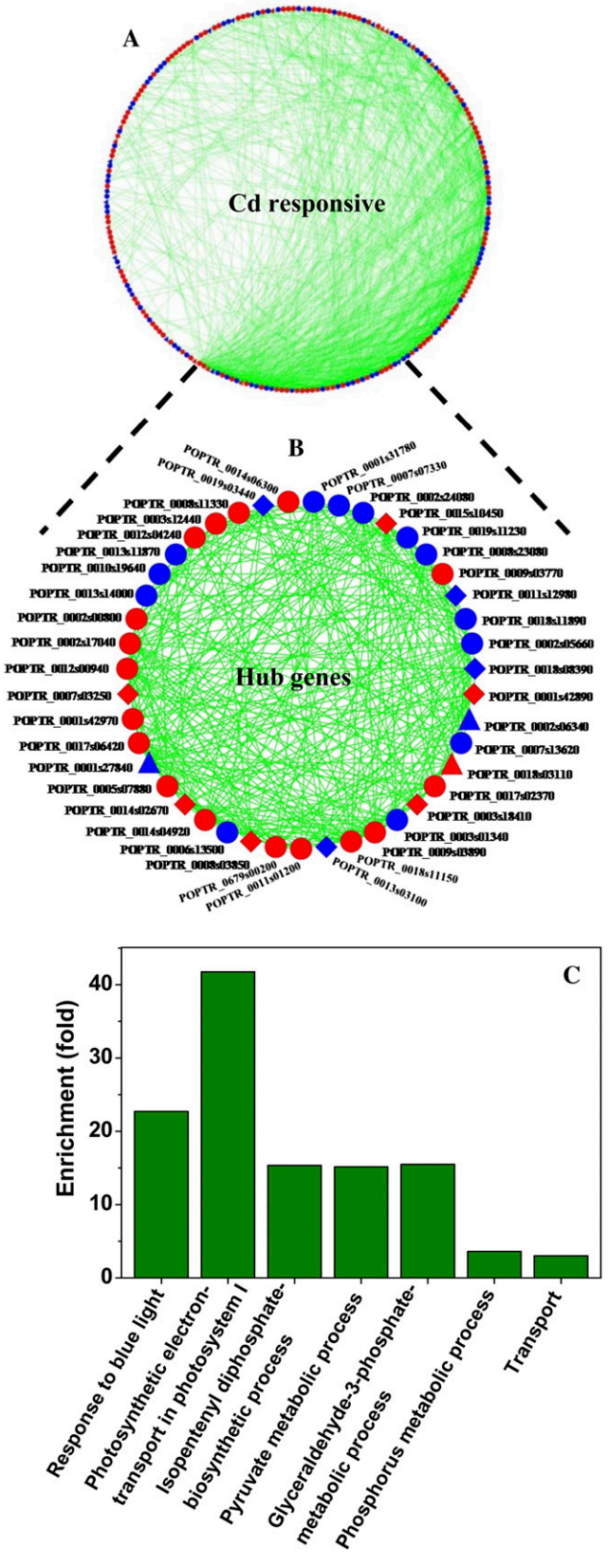

Figure 7. The coexpression network of significantly differentially expressed genes (A), the subnetwork of hub genes (B), and the GO term enrichment of hub genes (C) in the bark of *P.* × *canescens* exposed to 0 or 200 μM $CdSO_4$ for 20 d. The network was generated by setting a cutoff value of 0.15 for Kolmogorov-Smirnov quality-control statistics and an r^2 value of 0.36, which gives reliable results of coexpressed genes in CressExpress as suggested by Wei et al. (2006). An edge indicates the coexpression between two genes. Triangle nodes represent genes from the category of RNA regulation, diamond nodes represent genes from the signaling category, and circle nodes represent genes from other categories. Red and blue nodes represent up- and down-regulated genes, respectively. The presence of each node in the network and the hub genes (≥20 edges) are indicated in Supplemental Table S3. [See online article for color version of this figure.]

tissue, but not in root tissue (Fig. 8C). In agreement with overexpressed transcript level of the NADH-ubiquinone dehydrogenase6 involved in $O_2^{\bullet-}$ production (Raczynska et al., 2006; Supplemental Table S3), $O_2^{\bullet-}$ concentrations were markedly higher in the bark of cadmium-exposed *P.* × *canescens* (Supplemental Fig. S4). In addition, overall activation of GSH metabolism in the bark of cadmium-exposed *P.* × *canescens* was also consistent with up-regulation of the glutathione *S*-transferase involved in the conjugation of GSH (Supplemental Fig. S6; Supplemental Table S3).

Overall, the PCA results indicate that nutrients have a more distinct response pattern in bark than in either root or leaf tissue. By contrast, the response pattern of carbohydrates, oxidants, and antioxidants is similar in both bark and leaf tissue.

DISCUSSION

Vacuolar Sequestration and Apoplastic Binding Are the Microstructural Mechanisms for Cadmium Accumulation and Detoxification

Soil cadmium enters root xylem vessels via both apoplastic and symplastic pathways. The cadmium is carried upward by the transpiration stream and further transported to the bark through phloem loading (He et al., 2011; Mendoza-Cózatl et al., 2011). Although cadmium transport and accumulation are important in the phloem, no information is currently available about cadmium microlocalization in the bark (including the phloem) of woody plants (Vollenweider et al., 2006). In this study, cadmium microlocalization in the bark of *P.* × *canescens* was analyzed using several independent techniques (i.e. histochemical staining, TEM observation, and EDX analysis; Figs. 1–4). These data collectively confirm that *P.* × *canescens* can sequester cadmium in the phloem and highlight that the subcellular compartmentalization of cadmium occurs mainly in vacuoles.

Cadmium enters root cells via nutrient ion transporters and is further transported in the form of free ions in the xylem (Ueno et al., 2008). However, in the phloem sap of herbaceous plants, cadmium is mainly transported in the form of chelates with GSH and PCs

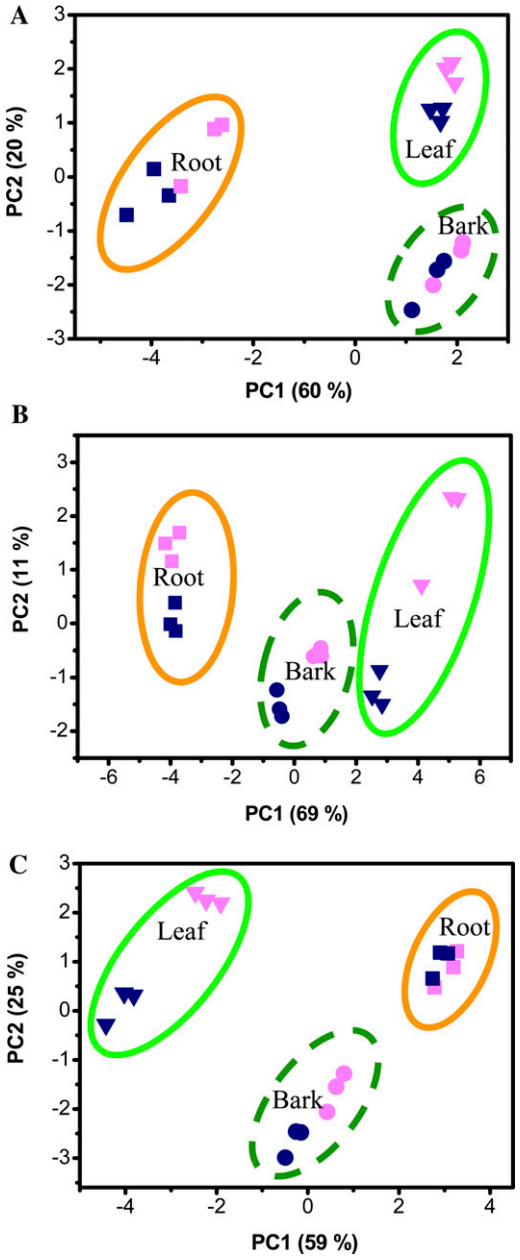

Figure 8. PCA plots of nutrients (A), soluble sugars and sugar alcohols (B), and oxidants and antioxidants (C) in the bark, fine roots, and leaves of *P.* × *canescens* exposed to 0 or 200 μM $CdSO_4$. Pink indicates 0 μM $CdSO_4$, and blue indicates 200 μM $CdSO_4$. PCA was conducted based on data (both values were averaged in the same tissue with the same treatment) presented in Supplemental Table S5 (A), Supplemental Table S6 (B), and Supplemental Figures S4 to S6 (C). [See online article for color version of this figure.]

(Mendoza-Cózatl et al., 2008). This may also be true in poplars, as indicated by cadmium accumulation and higher concentrations of thiols and sulfur in the bark of cadmium-exposed *P.* × *canescens*. After transport, cadmium-ligands reach vacuoles, and cadmium begins to accumulate (Mendoza-Cózatl et al., 2011). The accumulated cadmium may form cadmium granules, which are displayed as electron-dense particles under a transmission electron microscope (Van Belleghem et al., 2007). We observed that this also occurs in bark, suggesting massive plant internal cycling of cadmium. Moreover, correlation between cadmium and sulfur concentrations in cadmium granules indicates that cadmium may be immobilized with sulfur-containing compounds in vacuoles of cadmium-treated *P.* × *canescens*. Consistently, cadmium is found to be deposited with sulfur in Arabidopsis cells (Van Belleghem et al., 2007). Transport and vacuolar sequestration of cadmium-ligands (not free cadmium ions) in the phloem can minimize the damage of cadmium ions to physiologically functional cells or subcellular organelles in the phloem.

Although vacuolar sequestration of cadmium can minimize toxicity, damage to subcellular structures may occur because degeneration of chloroplasts, and mitochondria were observed in the bark of cadmium-exposed *P.* × *canescens* (Fig. 3). Structural changes such as the reduction of grana will decrease photosynthetic activity and thus result in reduced photosynthates (McCarthy et al., 2001; Mysliwa-Kurdziel et al., 2004). Actually, we observed fewer starch grains in companion cells and reduced carbohydrate concentrations in the bark of cadmium-exposed *P.* × *canescens* (Fig. 3; Supplemental Table S6). Mitochondria are also often injured by cadmium exposure in plant leaves (Lösch, 2004). In our study, the mitochondrial cristae of companion cells of cadmium-exposed *P.* × *canescens* were disorganized (Fig. 3). Cadmium-induced injury of the membrane systems in chloroplasts and mitochondria may give rise to lipid and protein degradation (see below).

In fine roots and leaves of *P.* × *canescens*, cadmium microlocalization was mainly confined to the apoplast and vacuoles, suggesting that compartmentation may play a critical role in cadmium accumulation and detoxification in woody plants. Cadmium precipitates are mainly located at the plasma membrane in Arabidopsis, (Van Belleghem et al., 2007), but not in pea (*Pisum sativum*; Romero-Puertas et al., 2004) or in *P.* × *canescens* (this study). Cadmium deposition in the vacuoles and cell walls of roots is typical for hyperaccumulators such as *A. halleri* and *T. caerulescens* (Vazquez et al., 1992; Küpper et al., 2000). *P.* × *canescens* can apparently utilize two strategies to maximize cadmium sequestration: (1) formation of an apoplast barrier by binding cadmium ions with cell walls and (2) symplastic sequestration by cadmium deposition in vacuoles. As a result, cadmium retention in roots may be maximized, reducing both cadmium entry into the central cylinder and cadmium transport to aerial parts. Once it reaches *P.* × *canescens* leaves, cadmium can be deposited in vacuoles of the mesophyll cells as observed in *A. halleri* (Küpper et al., 2000; Huguet et al., 2012). This suggests that *P.* × *canescens* leaves also use vacuolar sequestration to reduce cadmium toxicity.

The Coexpression Network Plays a Central Role in Transcriptomic Regulation Underlying the Microstructural and Physiological Responses to Cadmium

Although transcriptional profiles have been studied in cadmium-treated herbaceous plants, including Arabidopsis, *A. halleri*, *Solanum torvum*, *Solanum nigrum*, and rice (*Oryza sativa*; Herbette et al., 2006; Weber et al., 2006; Ogawa et al., 2009; Yamaguchi et al., 2010; Romero-Puertas et al., 2012; Xu et al., 2012) and in zinc-exposed *Populus* × *euramericana* (Di Baccio et al., 2011), no information is available about transcriptomic regulation underlying the microstructural responses to cadmium in woody plants. Cadmium accumulation in vacuoles of *P.* × *canescens* bark cells indicates that some transporters for heavy metals may be involved in this process. Vacuolar membrane-localized ATP-binding cassette (ABC) transporters of yeast (*Saccharomyces cerevisiae*) and Arabidopsis (ABC C type) are implicated in transport of cadmium-PCs and/or cadmium-bis-glutathione (Ortiz et al., 1995; Li et al., 1997; Park et al., 2012). In this study, increased transcript levels of two ABC transporters may contribute to cadmium accumulation in *P.* × *canescens* bark. These two *P.* × *canescens* ABC transporters belong to B- and G-type members (Verrier et al., 2008), and their function in cadmium transport remains to be studied. A heavy metal transport/detoxification superfamily protein and natural resistance-associated macrophage protein1 are involved in cadmium transport in Arabidopsis (Thomine et al., 2000; Wintz and Vulpe, 2002). The differential expression of these genes may also contribute to cadmium accumulation in *P.* × *canescens* bark cells. PSII subunit P-1 is involved in the development of normal thylakoid architecture (Yi et al., 2009), and a NADH-ubiquinone oxidoreductase-related gene affects the respiration process in mitochondria (Meyer et al., 2008); therefore, decreased transcript levels of both genes are probably associated with degeneration of chloroplasts and mitochondria in *P.* × *canescens* bark cells. Furthermore, damage to chloroplast grana and mitochondrial cristae in the bark of cadmium-exposed *P.* × *canescens* is probably linked with degradation of membrane lipids and proteins caused by overexpression of a number of genes (Supplemental Table S3). In fact, membrane proteolysis is induced in pea and poplar leaves exposed to cadmium (Romero-Puertas et al., 2002; Kieffer et al., 2008, 2009b). These findings indicate that some transcriptional changes may result from impaired metabolism due to cadmium toxicity in *P.* × *canescens* bark. Overall, these data highlight that transcriptomic regulation is associated with cadmium transport and vacuolar sequestration and with injury to chloroplasts and mitochondria in the bark of cadmium-exposed *P.* × *canescens*.

In the study, we have identified that transcriptomic responses to cadmium are involved in internal nutrient homeostasis, in carbohydrate metabolism, and in the balance of oxidants and antioxidants in *P.* × *canescens* bark. NRT2;4 is a plasma membrane nitrate transporter that is expressed in shoot phloem in response to external nitrogen concentrations (Kiba et al., 2012; Li et al., 2012). Phosphate transporters (PHT1;4 and PHT3;3) are involved in phosphorus signaling and transport in Arabidopsis (Morcuende et al., 2007; Lei et al., 2011). In *P.* × *canescens* bark, decreased expression of these genes may contribute to reductions in nitrogen and phosphorus concentrations under cadmium exposure. In cadmium-treated herbaceous plants, decreased transcripts levels of genes involved in photosynthesis and carbohydrate metabolism has been observed (Mysliwa-Kurdziel et al., 2004; Herbette et al., 2006; Weber et al., 2006; Ogawa et al., 2009; Yamaguchi et al., 2010; Sandalio et al., 2012; Xu et al., 2012). In cadmium-exposed *Populus tremula* leaves, repression of essential proteins involved in the photosystem, chlorophyll biosynthesis, and carbohydrate metabolism has been detected (Kieffer et al., 2008, 2009b). Because chloroplast-targeted alkaline/neutral invertase and chloroplastidic phosphoglucanase are involved in hydrolysis of Suc and starch, respectively (Hejazi et al., 2008; Tamoi et al., 2010), activation of both genes is in line with the changes in Suc and starch that we observed in the bark of cadmium-treated *P.* × *canescens*. In addition, decreased transcript levels of galactinol synthase1 and raffinose synthase5 may have contributed to the reductions in inositol and mannitol concentrations in the *P.* × *canescens* bark because both genes are involved in inositol and mannitol metabolism (Zuther et al., 2004; Nishizawa et al., 2008).

As a toxic heavy metal, cadmium can cause serious stress to plants. The stimulation of stress responses at the transcript level has often been reported in herbaceous plants (Herbette et al., 2006; Weber et al., 2006; Ogawa et al., 2009; Yamaguchi et al., 2010). We found a relatively high number of genes implicated in biotic stress in the bark of cadmium-exposed *P.* × *canescens*. Proteomic analysis revealed overexpression of pathogen-related proteins in cadmium-treated *P. tremula* (Kieffer et al., 2008, 2009b). In agreement with increased $O_2^{\bullet-}$ radicals, cadmium-exposed poplars exhibited an elevated transcript level of *NADH-ubiquinone dehydrogenase6*, which has been shown to result in increased oxidative stress (Raczynska et al., 2006). Thiols are often depleted under cadmium stress (Sharma and Dietz, 2009) and therefore may not have counterbalanced elevated radical production (Schützendübel and Polle, 2002).

Our data clearly demonstrate that transcriptomic reprogramming underlies the microstructural and physiological responses to cadmium accumulation and detoxification in *P.* × *canescens* bark. Furthermore, about one-half of the cadmium-responsive genes formed a coexpression network, indicating that *P.* × *canescens* coordinates the transcriptomic regulation for heavy metal stress. Recently, coregulation networks of transcriptomes have been reported in rice (Zhang et al., 2012), Arabidopsis (Bassel et al., 2011; Movahedi et al., 2011), pepper (*Capsicum annuum*), and tomato

(*Solanum lycopersicum*; Osorio et al., 2012), and maize (*Zea mays*; Ficklin and Feltus, 2011). However, none of these studies have addressed the coexpression of genes in response to cadmium in plants. For the first time, we have demonstrated the transcriptomic network underlying the microstructural and physiological responses to cadmium accumulation and detoxification in *P.* × *canescens* bark. Moreover, GO term analysis indicates that hub genes were enriched in fundamental processes such as transport and photosynthesis. These data suggest that the highly connected hub genes in the coexpression network play a central role in cross talk among distinct biological processes and in coordinating transcriptomic regulation in the bark of cadmium-exposed *P.* × *canescens*.

Changed Nutrient and Carbohydrate Concentrations and Shifted Homeostasis between ROS and the Antioxidants Highlight the Physiological Regulation Mechanism to Cadmium

The PCA of nutrients, carbohydrates, oxidants, and antioxidants and the assessment data of these physiological parameters in *P.* × *canescens* indicated that *P.* × *canescens* possess a physiological regulation mechanism to cadmium exposure. Previous studies reported that nitrogen and phosphorus are involved in detoxification of cadmium-exposed Arabidopsis (Van Belleghem et al., 2007; Li et al., 2010; Mendoza-Cózatl et al., 2011) and that decreased nitrogen and phosphorus are found in pea plants due to cadmium toxicity (Sandalio et al., 2001; Metwally et al., 2005). Bark nitrogen and phosphorus concentrations were consistently lower in cadmium-exposed *P.* × *canescens* than in the control, probably due to repressed nitrogen and phosphorus uptake. Sulfur-containing compounds (e.g. GSH and PCs) are used as chelates for cadmium (Herbette et al., 2006; Rodríguez-Serrano et al., 2009; Gill et al., 2012). Sulfur accumulation in the bark of cadmium-exposed *P.* × *canescens* is probably associated with accelerated biosynthesis of thiol compounds, such as GSH, to detoxify cadmium. The finding of decreases in calcium, iron, manganese, and zinc in cadmium-treated *P.* × *canescens* is consistent with previous studies (Sandalio et al., 2001; Metwally et al., 2005; Solti et al., 2008; Rodríguez-Serrano et al., 2009) and probably due to competition with cadmium ions for transporters. Reduction in CO_2 assimilation is probably due to defects in the photosynthetic apparatus (McCarthy et al., 2001; Solti et al., 2008; Ivanova et al., 2011), inactivation of photosynthesis-related enzymes (Leon et al., 2002; He et al., 2011), decreases in photosynthetic pigments or iron (Solti et al., 2008; Besson-Bard et al., 2009; Wu et al., 2012), and differential expression of photosynthesis-related genes and proteins (Kieffer et al., 2009a, 2009b; Durand et al., 2010). Reduced CO_2 assimilation often leads to changes in the concentrations of sugars and sugar alcohols in cadmium-treated plants (Devi et al., 2007; Kieffer et al., 2009a; He et al., 2011). Decreases in Suc, mannitol, inositol, and starch in *P.* × *canescens* bark are in agreement with inhibited photosynthesis under cadmium exposure. Accumulation of $O_2^{\bullet-}$ in bark and leaves and of H_2O_2 in leaves of cadmium-exposed *P.* × *canescens* suggests that oxidative stress occurs as observed in previous studies (Schützendübel et al., 2002; Romero-Puertas et al., 2004, 2012; Garnier et al., 2006; Rodríguez-Serrano et al., 2006, 2009; He et al., 2011). Oxidative burst is toxic for plant cells; therefore, excess ROS must be scavenged in cadmium-treated *P.* × *canescens*. Enzymatic antioxidants are proposed to play a role in ROS detoxification in cadmium-exposed plants (Leon et al., 2002; Gratao et al., 2005; Rodríguez-Serrano et al., 2006; Romero-Puertas et al., 2006, 2007; Elobeid et al., 2012); however, the activities of enzymatic antioxidants were unchanged or reduced by cadmium exposure in our study, indicating that the role of enzymatic antioxidants in ROS scavenging in cadmium-treated *P.* × *canescens* was limited. Notably, other antioxidants, such as free Pro, soluble phenolics, ascorbate, GSH, oxidized glutathione (GSSG), and total thiols, are involved in scavenging cadmium-induced $O_2^{\bullet-}$ and H_2O_2 (Sharma and Dietz, 2009). The induction of these antioxidants in cadmium-treated *P.* × *canescens* implies that these antioxidants play a pivotal role in scavenging excess ROS. The induction of these antioxidants, particularly thiols, and their role in cadmium detoxification have been documented in other plants (Vogel-Mikus et al., 2010; Gaudet et al., 2011; Seth et al., 2012). Overall, these data indicate that changes in internal nutrients, carbohydrates, and antioxidants play a role in physiological regulation of cadmium-exposed *P.* × *canescens*.

In conclusion, *P.* × *canescens* bark tissue accumulated cadmium about 2 times above the threshold of hyperaccumulation. Cadmium was translocated to the phloem in the bark, and subcellular cadmium compartmentalization in this tissue occurred mainly in vacuoles of phloem cells. Degeneration of chloroplasts and mitochondria took place in companion cells. Microstructural alterations, changes in nutrition and primary metabolism, and stimulation of stress responses in cadmium-exposed bark were mirrored by differential expression of genes related to these processes. About one-half of the differentially regulated transcripts formed a coregulation network in which 43 hub genes may play a central role both in cross talk among distinct biological processes and in coordinating the transcriptomic regulation in the bark of *P.* × *canescens*. In concert, these results suggest that orchestrated microstructural, transcriptomic, and physiological regulation can be essential for cadmium accumulation and detoxification in *P.* × *canescens* and provide new insights into engineering woody plants for phytoremediation.

MATERIALS AND METHODS

Cultivation of Plants and Cadmium Exposure

Plantlets of *Populus* × *canescens* (*Populus tremula* × *Populus alba*) were produced by micropropagation (Leple et al., 1992) and cultivated in a climate

chamber (day/night temperature, 25°C/18°C; relative air humidity, 50%–60%; photoperiod, 14 h; photosynthetic photon flux, 150 μmol m^{-2} s^{-1}). After 5 weeks, the rooted plantlets were transferred to 10-L plastic pots filled with 10 kg of sand. Plants were cultivated for 10 weeks in a greenhouse (day/night temperature, 25°C /18°C; relative air humidity, 50%–60%; natural light) before cadmium exposure. Nutrient solution (30 mL full-strength Hoagland solution) was slowly added to the pots each morning. Water (30 mL) was added each evening. Twenty-four plants with similar height were selected and divided into two groups, with 12 plants in each group: one group for the cadmium treatment (200 μM $CdSO_4$) and the other for the control (0 μM $CdSO_4$). Plants were grown for 20 d in the absence or presence of cadmium, which was supplied daily with the nutrient solution before harvest.

Gas Exchange Measurement and Harvest

Before harvest, three mature leaves (leaf plastochron index [Erickson and Michelini, 1957] = 7–9) were selected from each plant for gas exchange measurements. Net photosynthetic rate, stomatal conductance, and transpiration rate were determined using a portable photosynthesis system (LiCor-6400) as described previously (He et al., 2011).

After measuring photosynthesis, the root system of each plant was carefully washed as suggested by Rauser (1987). Subsequently, the roots and aboveground tissues of each plant were harvested. The aboveground tissues were separated into bark, wood, and leaves. The samples were weighed (fresh weight), wrapped with tinfoil, and immediately frozen in liquid nitrogen. Frozen samples were ground into fine powder in liquid nitrogen with a mortar and a pestle and stored at −80°C for further analysis. Fresh powder (approximately 30 mg) of each tissue from each plant was separately dried at 60°C to determine the fresh-to-dry mass ratio. This ratio was used to calculate the dry weight (biomass) of each tissue. An equal amount of fine powder from two plants in each treatment was combined and thoroughly mixed for biochemical analysis. Fine powder of bark tissue from four plants in each treatment was thoroughly mixed and used for RNA extraction. Subsamples of fine roots, stems, petioles, and leaves were also harvested for anatomical and histochemical analysis.

Analysis of Cadmium, Nutrient Elements, and Foliar Pigments

Concentrations of cadmium and zinc were determined in roots, bark, and leaves by flame atomic absorbance spectrometry (Hitachi 180-80) as described by He et al. (2011). Total carbon and nitrogen in different tissues were analyzed with a carbon/nitrogen analyzer (Elemental Analyzer EA1108, Carlo Erba Strumentazione) as described in Luo and Polle (2009). Mineral elements were determined using an inductively coupled plasma-atomic emission spectrometer (Spectroflame, Spectro Analytical Instruments) based on the protocol described by Luo et al. (2009a). Chlorophyll and carotenoid contents in leaves were determined spectrophotometrically as suggested by He et al. (2013).

Cadmium Localization at Tissue and Subcellular Levels

To characterize cadmium localization at the tissue level, hand sections or intact tissues of fresh samples of fine roots, stems, petioles, and leaves were rinsed in deionized water, subsequently exposed to a staining solution (30 mg diphenylthiocarbazone in 60 mL acetone, 20 mL water, 100 μL glacial acetic acid) for 1 h, and then briefly rinsed in deionized water as suggested by Clabeaux et al. (2011). Well-stained samples with cadmium-dithizone precipitates displaying red-black were photographed under a light microscope (Eclipse E200, Nikon) with a CCD (DS-Fi1, Nikon) connected to a computer as described by Cao et al. (2012).

To further characterize cadmium localization at the subcellular level, samples were prepared for TEM as suggested by Gratao et al. (2009) with minor modifications. Briefly, samples of fine roots, bark, and leaves were cut into sections (approximately 1–2 mm^3), fixed with 4% (v/v) glutaraldehyde in 0.1 M phosphate buffer (pH 6.8) at 4°C overnight, and subsequently washed three times with phosphate buffer (0.1 M, pH 6.8). The samples were then fixed with 1% (w/v) osmium tetroxide for 2 h and immersed in 0.1 M phosphate buffer (pH 6.8) for 1 h. The sections were dehydrated in a graded ethanol series (30%, 50%, 70%, 80%, 90%, and 100%, v/v) with 10- to 20-min intervals, infiltrated, and embedded in Epon resin. Ultrathin (70 nm) were collected on copper grids and stained with 2.5% (w/v) uranyl acetate followed by 0.1% (w/v) lead citrate. Sections were photographed under a transmission electron microscope (HT7700, Hitachi) at 75 kV.

To examine cadmium contents in the granular deposits, EDX microanalysis was carried out on ultrathin sections (no staining with 2.5% [w/v] uranyl acetate and 0.1% [w/v] lead citrate) of different tissues as proposed by Van Belleghem et al. (2007). The transmission electron microscope was equipped with an EDX detector (Genesis XM2, EDAX). The sections were analyzed at an accelerating voltage of 80 kV. The EDX spectra with cadmium Lα (3.133 keV) and sulfur Kα (2.308 keV) were recorded during an analysis period of 200 live seconds (total spectrum collection time). Spectra analyses were conducted using the SuperQuant program (EDAX). The measurement parameters (section thickness, beam emission current, spot diameter, and tilt angle) were constant throughout the analyses. The cadmium concentrations in granular deposits were expressed as the ratio between the specific emission intensity of cadmium above background and the nonspecific emission intensity of the background (peak/background).

RNA Extraction and DNA Chip Hybridization

Fine powder of bark (approximately 500 mg) was used for RNA extraction according to Chang et al. (1993) with minor modifications described previously (Luo et al., 2009a). The extraction buffer contained 2% (v/v) β-mercaptoethanol and no spermidine. The RNA was purified (RNeasy Mini Kit, Qiagen). The purity and integrity of the RNA were assessed according to the Affymetrix GeneChip expression analysis protocol. Further processing of the RNA and complementary RNA hybridization using the Affymetrix poplar (*Populus* spp.) genome array were accomplished at the microarray service facilities of the Shanghai Biotechnology Company. For each treatment, three arrays were hybridized, thus yielding six arrays. Raw data of the arrays are available at the ArrayExpress depository (http://www.ebi.ac.uk/arrayexpress/; accession no. E-MEXP-3741).

Annotation, Functional Categorization, Coexpression, and GO Enrichment Analysis

To obtain up-to-date annotations of differentially expressed genes, we performed several BLAST searches as described by Janz et al. (2012). Briefly, the Affymetrix GeneChip poplar genome array target sequences were used to blast (BLASTn) against the Phytozome *Populus trichocarpa* version 2.2 transcript database. The closest Arabidopsis (*Arabidopsis thaliana*) homolog (AGI identification) of a *P.* × *canescens* gene was determined by a translated nucleotide BLAST (BLASTx) of the coding sequence of the best *P. trichocarpa* hit against the Arabidopsis protein sequence data set. Annotations were taken from the latest release of The Arabidopsis Information Resource genome, TAIR10.

To categorize differentially expressed genes based on their biological functions, *P.* × *canescens* genes with unique AGIs (only the *P.* × *canescens* gene with the lowest *P* value in Supplemental Table S2 was selected when multiple *P.* × *canescens* genes corresponded to an AGI) were selected and submitted to MapMan for analysis as suggested by Thimm et al. (2004). Subsequently, all genes with functional categorization and subsets of genes assigned to categories of photosynthesis, stress, RNA regulation (mainly transcription factors), signaling, and transport by MapMan were used for coexpression analysis as described by Wei et al. (2006), using an online open resource (http://cressexpress.org/index.jsp). Results of coexpression analysis were visualized in Cytoscape version 2.8.3 as described by Shannon et al. (2003).

To perform GO term enrichment analyses for all cadmium-responsive genes, coexpressed genes, and hub genes, AGIs of these genes were used for singular enrichment analysis in the agriGO database (http://bioinfo.cau.edu.cn/agriGO/analysis.php) as suggested by Du et al. (2010).

Validation of Microarray Analysis by Quantitative RT-PCR

Total RNA of bark was isolated and purified with a plant RNA extraction kit (R6827, Omega Bio-Tek). Quantitative reverse transcription (RT)-PCR of seven genes (for primer information, see Supplemental Table S8) was performed according to Li et al. (2012). The reference gene was 18S ribosomal RNA (Supplemental Table S8). To ensure the specification, PCR products were sequenced and aligned with the homologs in other model plants (Supplemental Fig. S7). The correlation of gene expression was analyzed between the microarray and the quantitative RT-PCR data (Supplemental Fig. S8).

Analysis of Soluble Sugars, Sugar Alcohols, and Starch

Soluble sugars and sugar alcohols were determined by gas chromatography-mass spectrometry as described previously (Luo et al., 2009a, 2009b). Starch concentrations (expressed as Glc equivalent) in samples were analyzed using the anthrone method described by He et al. (2013). Absorption was determined spectrophotometrically at 620 nm.

Determination of $O_2^{\bullet-}$ and H_2O_2

Concentrations of $O_2^{\bullet-}$ and H_2O_2 in samples were determined spectrophotometrically at 530 and 410 nm, respectively, as described previously (Martínez Domínguez et al., 2010; He et al., 2011). For $O_2^{\bullet-}$ determination, fine powder of fresh tissues (approximately 100 mg) was homogenized in 2 mL of 50 mM potassium phosphate buffer (pH 7.8) and centrifuged at 10,000*g* and 4°C for 10 min. The supernatant (1 mL) was mixed with 0.9 mL of 50 mM potassium phosphate buffer (pH 7.8) and 0.1 mL of 10 mM hydroxylamine hydrochloride. The reaction mixture was then incubated at 25°C for 20 min before adding 1 mL of 17 mM *P*-aminobenzene sulfonic acid and 1 mL of 7 mM α-naphthylamine. After further incubation at 25°C for 20 min, the absorbance of the mixture was recorded spectrophotometrically at 530 nm.

To determine H_2O_2 concentrations, the fine powder of fresh tissue (approximately 60 mg) was extracted in 2 mL acetocaustin and centrifuged at 10,000*g* and 4°C for 10 min. The supernatant was collected. After adding 0.1 mL of 20% (v/v) $TiCl_4$ and 0.2 mL of 25% (v/v) aqueous ammonia to the supernatant, the mixture was immediately centrifuged again at 10,000*g* and 4°C for 10 min. The supernatant was then discarded, and the pellet was dissolved in 3 mL of 1 M H_2SO_4. The absorbance was recorded spectrophotometrically at 410 nm.

Analysis of Enzyme Activities, Pro, and Soluble Phenolics

Soluble proteins were extracted and used for assays of enzyme activities as described previously by He et al. (2011).

Free Pro was determined spectrophotometrically according to He et al. (2011). The standard curve was generated using a series of diluted L-Pro solutions (Amresco).

Soluble phenolics in samples were determined spectrophotometrically by using the Folin-Ciocalteu reagent as reported by Luo et al. (2008). A standard curve was prepared using a series of diluted catechin solutions (Sigma).

Analysis of Ascorbate, GSH, GSSG, and Total Thiols

Ascorbate was analyzed based on the protocol described by Chen et al. (2011) with minor modifications. Plant samples (approximately 100 mg) were extracted in 6% (w/v) TCA (prechilled on ice) and centrifuged at 12,000*g* and 4°C for 10 min. The supernatant was analyzed spectrophotometrically at 525 nm.

GSH and GSSG were analyzed using the 5,5′-dithiobis(2-nitrobenzoic acid)-glutathione reductase recycling procedure suggested by Chen et al. (2011).

Total thiols were analyzed according to Tamás et al. (2008) with minor modifications. Freeze-dried tissues (approximately 100 mg) were extracted in 1 mL of 20 mM EDTA on ice and centrifuged at 12,000*g* and 4°C for 10 min. A 0.25-mL aliquot of the supernatant was mixed with 2.5 mL of Tris buffer (0.2 M, pH 8.2) and 50 μL of 10 mM 5,5′-dithiobis(2-nitrobenzoic acid). After incubation at room temperature for 15 min, the absorbance of the reaction mixture was determined spectrophotometrically at 412 nm.

Statistical Analysis

Statistical tests were performed with Statgraphics (STN). For experimental variables, one-way ANOVA was applied with cadmium treatment as a factor. Data were tested for normality prior to the statistical analysis. Differences between means were considered significant when the *P* value of the ANOVA *F* test was less than 0.05. For PCA, data were standardized and subsequently computed by the command prcomp() in R (http://www.r-project.org/).

For microarray analysis, raw probe intensity values from the Affymetrix CEL files generated at the microarray service facilities were analyzed in an SBC Analysis System (http://sas.ebioservice.com) as described by Li et al. (2011), which was developed based on algorithms in R package (http://www.r-project.org/). Background correction and quantile normalization of raw data were computed by the rma algorithm from the affy package (Irizarry et al., 2003). Subsequently, differentially expressed genes (cadmium-treated versus control group) were identified from background-corrected and normalized data by one-way ANOVA with *P* values less than 0.05. Relative expression ratios of selected genes for quantitative RT-PCR were determined using the Relative Expression Software Tool (Pfaffl et al., 2002).

Supplemental Data

The following materials are available in the online version of this article.

Supplemental Figure S1. Cadmium localization in petioles and leaves.

Supplemental Figure S2. EDX spectra of granular deposits in vacuoles of bark cells.

Supplemental Figure S3. Transmission electron microscopic micrographs.

Supplemental Figure S4. $O_2^{\bullet-}$ and H_2O_2 in the bark, root, and leaf tissues.

Supplemental Figure S5. Activities of antioxidant enzymes.

Supplemental Figure S6. Nonenzymatic antioxidants.

Supplemental Figure S7. Alignments of genes for quantitative RT-PCR.

Supplemental Figure S8. Correlation of gene expression between the microarray and quantitative RT-PCR data.

Supplemental Table S1. Photosynthesis and biomass.

Supplemental Table S2. Significantly differentially regulated transcripts.

Supplemental Table S3. Functional categories of genes and gene presence in the coexpression network.

Supplemental Table S4. GO term enrichment analysis.

Supplemental Table S5. Total nitrogen, carbon, and nutrients.

Supplemental Table S6. Carbohydrate concentrations.

Supplemental Table S7. PCA of nutrients, carbohydrates, oxidants, and antioxidants.

Supplemental Table S8. Primers used for quantitative RT-PCR.

ACKNOWLEDGMENTS

We thank Christine Kettner and Gisbert Langer-Kettner for nutrient element analysis, William J. Gale for English correction, and anonymous reviewers for their suggestions to improve the manuscript.

Received February 1, 2013; accepted March 22, 2013; published March 25, 2013.

LITERATURE CITED

Ager FJ, Ynsa MD, Dominguez-Solis JR, Lopez-Martin MC, Gotor C, Romero LC (2003) Nuclear micro-probe analysis of *Arabidopsis thaliana* leaves. Nucl Instrum Methods Phys Res B **210:** 401–406

Bassel GW, Glaab E, Marquez J, Holdsworth MJ, Bacardit J (2011) Functional network construction in *Arabidopsis* using rule-based machine learning on large-scale data sets. Plant Cell **23:** 3101–3116

Bertin G, Averbeck D (2006) Cadmium: cellular effects, modifications of biomolecules, modulation of DNA repair and genotoxic consequences (a review). Biochimie **88:** 1549–1559

Besson-Bard A, Gravot A, Richaud P, Auroy P, Duc C, Gaymard F, Taconnat L, Renou JP, Pugin A, Wendehenne D (2009) Nitric oxide contributes to cadmium toxicity in Arabidopsis by promoting cadmium accumulation in roots and by up-regulating genes related to iron uptake. Plant Physiol **149:** 1302–1315

Cao X, Jia JB, Li H, Li MC, Luo J, Liang ZS, Liu TX, Liu WG, Peng CH, Luo ZB (2012) Photosynthesis, water use efficiency and stable carbon isotope composition are associated with anatomical properties of leaf and xylem in six poplar species. Plant Biol (Stuttg) **14:** 612–620

Chang SJ, Puryear J, Cairney J (1993) A simple and efficient method for isolating RNA from pine trees. Plant Mol Biol Rep **11:** 113–116

Chen LH, Han Y, Jiang H, Korpelainen H, Li CY (2011) Nitrogen nutrient status induces sexual differences in responses to cadmium in *Populus yunnanensis*. J Exp Bot **62:** 5037–5050

Clabeaux BL, Navarro DAG, Aga DS, Bisson MA (2011) Cd tolerance and accumulation in the aquatic macrophyte, *Chara australis*: potential use for charophytes in phytoremediation. Environ Sci Technol **45:** 5332–5338

Conn S, Gilliham M (2010) Comparative physiology of elemental distributions in plants. Ann Bot (Lond) **105:** 1081–1102

Cunha KP, do Nascimento CWA, Pimentel RMD, Ferreira CP (2008) Cellular localization of cadmium and structural changes in maize plants grown on a cadmium contaminated soil with and without liming. J Hazard Mater **160:** 228–234

Davies PJ (2010) The plant hormones: their nature, occurrence, and functions. *In* **Davies PJ**, ed, Plant Hormones. Springer, Berlin, pp 1–15

Devi R, Munjral N, Gupta AK, Kaur N (2007) Cadmium induced changes in carbohydrate status and enzymes of carbohydrate metabolism, glycolysis and pentose phosphate pathway in pea. Environ Exp Bot **61:** 167–174

Di Baccio D, Galla G, Bracci T, Andreucci A, Barcaccia G, Tognetti R, Sebastiani L (2011) Transcriptome analyses of *Populus* × *euramericana* clone I-214 leaves exposed to excess zinc. Tree Physiol **31:** 1293–1308

Du Z, Zhou X, Ling Y, Zhang ZH, Su Z (2010) agriGO: a GO analysis toolkit for the agricultural community. Nucleic Acids Res **38:** W64–W70

Durand TC, Sergeant K, Planchon S, Carpin S, Label P, Morabito D, Hausman JF, Renaut J (2010) Acute metal stress in *Populus tremula* × *P. alba* (717-1B4 genotype): leaf and cambial proteome changes induced by cadmium^{2+}. Proteomics **10:** 349–368

Elobeid M, Göbel C, Feussner I, Polle A (2012) Cadmium interferes with auxin physiology and lignification in poplar. J Exp Bot **63:** 1413–1421

Erickson RO, Michelini FJ (1957) The plastochron index. Am J Bot **44:** 297–305

Ficklin SP, Feltus FA (2011) Gene coexpression network alignment and conservation of gene modules between two grass species: maize and rice. Plant Physiol **156:** 1244–1256

Garnier L, Simon-Plas F, Thuleau P, Agnel JP, Blein JP, Ranjeva R, Montillet JL (2006) Cadmium affects tobacco cells by a series of three waves of reactive oxygen species that contribute to cytotoxicity. Plant Cell Environ **29:** 1956–1969

Gaudet M, Pietrini F, Beritognolo I, Iori V, Zacchini M, Massacci A, Mugnozza GS, Sabatti M (2011) Intraspecific variation of physiological and molecular response to cadmium stress in *Populus nigra* L. Tree Physiol **31:** 1309–1318

Gill SS, Khan NA, Tuteja N (2012) Cadmium at high dose perturbs growth, photosynthesis and nitrogen metabolism while at low dose it up regulates sulfur assimilation and antioxidant machinery in garden cress (*Lepidium sativum* L.). Plant Sci **182:** 112–120

Gratao PL, Monteiro CC, Rossi ML, Martinelli AP, Peres LEP, Medici LO, Lea PJ, Azevedo RA (2009) Differential ultrastructural changes in tomato hormonal mutants exposed to cadmium. Environ Exp Bot **67:** 387–394

Gratao PL, Polle A, Lea PJ, Azevedo RA (2005) Making the life of heavy metal-stressed plants a little easier. Funct Plant Biol **32:** 481–494

He JL, Ma CF, Ma YL, Li H, Kang JQ, Liu TX, Polle A, Peng CH, Luo ZB (2013) Cadmium tolerance in six poplar species. Environ Sci Pollut Res Int **20:** 163–174

He JL, Qin JJ, Long LY, Ma YL, Li H, Li K, Jiang XN, Liu TX, Polle A, Liang ZS, et al (2011) Net cadmium flux and accumulation reveal tissue-specific oxidative stress and detoxification in *Populus* × *canescens*. Physiol Plant **143:** 50–63

Hejazi M, Fettke J, Haebel S, Edner C, Paris O, Frohberg C, Steup M, Ritte G (2008) Glucan, water dikinase phosphorylates crystalline maltodextrins and thereby initiates solubilization. Plant J **55:** 323–334

Herbette S, Taconnat L, Hugouvieux V, Piette L, Magniette MLM, Cuine S, Auroy P, Richaud P, Forestier C, Bourguignon J, et al (2006) Genome-wide transcriptome profiling of the early cadmium response of *Arabidopsis* roots and shoots. Biochimie **88:** 1751–1765

Heyndrickx KS, Vandepoele K (2012) Systematic identification of functional plant modules through the integration of complementary data sources. Plant Physiol **159:** 884–901

Huguet S, Bert V, Laboudigue A, Barthes V, Isaure MP, Llorens I, Schat H, Sarret G (2012) Cd speciation and localization in the hyperaccumulator *Arabidopsis halleri*. Environ Exp Bot **82:** 54–65

Irizarry RA, Hobbs B, Collin F, Beazer-Barclay YD, Antonellis KJ, Scherf U, Speed TP (2003) Exploration, normalization, and summaries of high density oligonucleotide array probe level data. Biostatistics **4:** 249–264

Ivanova LA, Ronzhina DA, Ivanov LA, Stroukova LV, Peuke AD, Rennenberg H (2011) Over-expression of *gsh1* in the cytosol affects the photosynthetic apparatus and improves the performance of transgenic poplars on heavy metal-contaminated soil. Plant Biol (Stuttg) **13:** 649–659

Janz D, Lautner S, Wildhagen H, Behnke K, Schnitzler JP, Rennenberg H, Fromm J, Polle A (2012) Salt stress induces the formation of a novel type of 'pressure wood' in two *Populus* species. New Phytol **194:** 129–141

Kiba T, Feria-Bourrellier AB, Lafouge F, Lezhneva L, Boutet-Mercey S, Orsel M, Bréhaut V, Miller A, Daniel-Vedele F, Sakakibara H, et al (2012) The *Arabidopsis* nitrate transporter NRT2.4 plays a double role in roots and shoots of nitrogen-starved plants. Plant Cell **24:** 245–258

Kieffer P, Dommes J, Hoffmann L, Hausman JF, Renaut J (2008) Quantitative changes in protein expression of cadmium-exposed poplar plants. Proteomics **8:** 2514–2530

Kieffer P, Planchon S, Oufir M, Ziebel J, Dommes J, Hoffmann L, Hausman JF, Renaut J (2009a) Combining proteomics and metabolite analyses to unravel cadmium stress-response in poplar leaves. J Proteome Res **8:** 400–417

Kieffer P, Schröder P, Dommes J, Hoffmann L, Renaut J, Hausman JF (2009b) Proteomic and enzymatic response of poplar to cadmium stress. J Proteomics **72:** 379–396

Kramer U (2010) Metal hyperaccumulation in plants. *In* **Merchant S, Briggs WR, Ort D**, eds, Annual Review of Plant Biology, **Vol 61**. Annual Reviews, Palo Alto, CA, pp 517–534

Küpper H, Kochian LV (2010) Transcriptional regulation of metal transport genes and mineral nutrition during acclimatization to cadmium and zinc in the Cd/Zn hyperaccumulator, *Thlaspi caerulescens* (Ganges population). New Phytol **185:** 114–129

Küpper H, Lombi E, Zhao FJ, McGrath SP (2000) Cellular compartmentation of cadmium and zinc in relation to other elements in the hyperaccumulator *Arabidopsis halleri*. Planta **212:** 75–84

Lei MG, Zhu CM, Liu YD, Karthikeyan AS, Bressan RA, Raghothama KG, Liu D (2011) Ethylene signalling is involved in regulation of phosphate starvation-induced gene expression and production of acid phosphatases and anthocyanin in Arabidopsis. New Phytol **189:** 1084–1095

Leon AM, Palma JM, Corpas FJ, Gomez M, Romero-Puertas MC, Chatterjee D, Mateos RM, del Rio LA, Sandalio LM (2002) Antioxidative enzymes in cultivars of pepper plants with different sensitivity to cadmium. Plant Physiol Biochem **40:** 813–820

Leple JC, Brasileiro ACM, Michel MF, Delmotte F, Jouanin L (1992) Transgenic poplars: expression of chimeric genes using four different constructs. Plant Cell Rep **11:** 137–141

Li H, Li M, Luo J, Cao X, Qu L, Gai Y, Jiang X, Liu T, Bai H, Janz D, et al (2012) N-fertilization has different effects on the growth, carbon and nitrogen physiology, and wood properties of slow- and fast-growing *Populus* species. J Exp Bot **63:** 6173–6185

Li JY, Fu YL, Pike SM, Bao J, Tian W, Zhang Y, Chen CZ, Zhang Y, Li HM, Huang J, et al (2010) The *Arabidopsis* nitrate transporter NRT1.8 functions in nitrate removal from the xylem sap and mediates cadmium tolerance. Plant Cell **22:** 1633–1646

Li KC, Zhang FX, Li CL, Wang F, Yu MY, Zhong YQ, Zhang KH, Lu YJ, Wang QO, Ma XL, et al (2011) Follistatin-like 1 suppresses sensory afferent transmission by activating Na^+,K^+-ATPase. Neuron **69:** 974–987

Li ZS, Lu YP, Zhen RG, Szczypka M, Thiele DJ, Rea PA (1997) A new pathway for vacuolar cadmium sequestration in *Saccharomyces cerevisiae*: YCF1-catalyzed transport of bis(glutathionato)cadmium. Proc Natl Acad Sci USA **94:** 42–47

Lösch R (2004) Plant mitochondrial respiration under the influence of heavy metals. *In* **Prasad MNV**, ed, Heavy Metal Stress in Plants From Biomolecules to Ecosystems. Springer-Verlag, Berlin, pp 182–200

Luo ZB, Calfapietra C, Scarascia-Mugnozza G, Liberloo M, Polle A (2008) Carbon-based secondary metabolites and internal nitrogen pools in *Populus nigra* under Free Air CO_2 Enrichment (FACE) and nitrogen fertilisation. Plant Soil **304:** 45–57

Luo ZB, Janz D, Jiang XN, Göbel C, Wildhagen H, Tan YP, Rennenberg H, Feussner I, Polle A (2009a) Upgrading root physiology for stress tolerance by ectomycorrhizas: insights from metabolite and transcriptional

profiling into reprogramming for stress anticipation. Plant Physiol **151:** 1902–1917

Luo ZB, Li K, Jiang XN, Polle A (2009b) Ectomycorrhizal fungus (*Paxillus involutus*) and hydrogels affect performance of *Populus euphratica* exposed to drought stress. Ann Sci **66:** 106

Luo ZB, Polle A (2009) Wood composition and energy content in a poplar short rotation plantation on fertilized agricultural land in a future CO_2 atmosphere. Glob Change Biol **15:** 38–47

Martínez Domínguez D, Córdoba García F, Canalejo Raya A, Torronteras Santiago R (2010) Cadmium-induced oxidative stress and the response of the antioxidative defense system in *Spartina densiflora*. Physiol Plant **139:** 289–302

McCarthy I, Romero-Puertas MC, Palma JM, Sandalio LM, Corpas FJ, Gomez M, Del Rio LA (2001) Cadmium induces senescence symptoms in leaf peroxisomes of pea plants. Plant Cell Environ **24:** 1065–1073

Mendoza-Cózatl DG, Butko E, Springer F, Torpey JW, Komives EA, Kehr J, Schroeder JI (2008) Identification of high levels of phytochelatins, glutathione and cadmium in the phloem sap of *Brassica napus*. A role for thiol-peptides in the long-distance transport of cadmium and the effect of cadmium on iron translocation. Plant J **54:** 249–259

Mendoza-Cózatl DG, Jobe TO, Hauser F, Schroeder JI (2011) Long-distance transport, vacuolar sequestration, tolerance, and transcriptional responses induced by cadmium and arsenic. Curr Opin Plant Biol **14:** 554–562

Merkle SA (2006) Engineering forest trees with heavy metal resistance genes. Silvae Genet **55:** 263–268

Metwally A, Safronova VI, Belimov AA, Dietz KJ (2005) Genotypic variation of the response to cadmium toxicity in *Pisum sativum* L. J Exp Bot **56:** 167–178

Meyer EH, Taylor NL, Millar AH (2008) Resolving and identifying protein components of plant mitochondrial respiratory complexes using three dimensions of gel electrophoresis. J Proteome Res **7:** 786–794

Milner MJ, Kochian LV (2008) Investigating heavy-metal hyperaccumulation using *Thlaspi caerulescens* as a model system. Ann Bot (Lond) **102:** 3–13

Morcuende R, Bari R, Gibon Y, Zheng WM, Pant BD, Bläsing O, Usadel B, Czechowski T, Udvardi MK, Stitt M, et al (2007) Genome-wide reprogramming of metabolism and regulatory networks of Arabidopsis in response to phosphorus. Plant Cell Environ **30:** 85–112

Movahedi S, Van de Peer Y, Vandepoele K (2011) Comparative network analysis reveals that tissue specificity and gene function are important factors influencing the mode of expression evolution in Arabidopsis and rice. Plant Physiol **156:** 1316–1330

Mysliwa-Kurdziel B, Prasad MNV, Stralka K (2004) Photosynthesis in heavy metal stressed plants. *In* **Prasad MNV**, ed, Heavy Metal Stress in Plants From Biomolecules to Ecosystems. Springer-Verlag, Berlin, pp 146–181

Nawrot T, Plusquin M, Hogervorst J, Roels HA, Celis H, Thijs L, Vangronsveld J, Van Hecke E, Staessen JA (2006) Environmental exposure to cadmium and risk of cancer: a prospective population-based study. Lancet Oncol **7:** 119–126

Nishizawa A, Yabuta Y, Shigeoka S (2008) Galactinol and raffinose constitute a novel function to protect plants from oxidative damage. Plant Physiol **147:** 1251–1263

Ogawa I, Nakanishi H, Mori S, Nishizawa NK (2009) Time course analysis of gene regulation under cadmium stress in rice. Plant Soil **325:** 97–108

Ortiz DF, Ruscitti T, McCue KF, Ow DW (1995) Transport of metal-binding peptides by HMT1, a fission yeast ABC-type vacuolar membrane protein. J Biol Chem **270:** 4721–4728

Osorio S, Alba R, Nikoloski Z, Kochevenko A, Fernie AR, Giovannoni JJ (2012) Integrative comparative analyses of transcript and metabolite profiles from pepper and tomato ripening and development stages uncovers species-specific patterns of network regulatory behavior. Plant Physiol **159:** 1713–1729

Park J, Song WY, Ko D, Eom Y, Hansen TH, Schiller M, Lee TG, Martinoia E, Lee Y (2012) The phytochelatin transporters AtABCC1 and AtABCC2 mediate tolerance to cadmium and mercury. Plant J **69:** 278–288

Pfaffl MW, Horgan GW, Dempfle L (2002) Relative expression software tool (REST©) for group-wise comparison and statistical analysis of relative expression results in real-time PCR. Nucleic Acids Res **30:** e36

Raczynska KD, Le Ret M, Rurek M, Bonnard G, Augustyniak H, Gualberto JM (2006) Plant mitochondrial genes can be expressed from mRNAs lacking stop codons. FEBS Lett **580:** 5641–5646

Rauser WE (1987) Compartmental efflux analysis and removal of extracellular cadmium from roots. Plant Physiol **85:** 62–65

Rodríguez-Serrano M, Romero-Puertas MC, Pazmiño DM, Testillano PS, Risueño MC, Del Río LA, Sandalio LM (2009) Cellular response of pea plants to cadmium toxicity: cross talk between reactive oxygen species, nitric oxide, and calcium. Plant Physiol **150:** 229–243

Rodríguez-Serrano M, Romero-Puertas MC, Zabalza A, Corpas FJ, Gómez M, Del Río LA, Sandalio LM (2006) Cadmium effect on oxidative metabolism of pea (*Pisum sativum* L.) roots. Imaging of reactive oxygen species and nitric oxide accumulation in vivo. Plant Cell Environ **29:** 1532–1544

Romero-Puertas MC, Corpas FJ, Rodríguez-Serrano M, Gómez M, Del Río LA, Sandalio LM (2007) Differential expression and regulation of antioxidative enzymes by cadmium in pea plants. J Plant Physiol **164:** 1346–1357

Romero-Puertas MC, Corpas FJ, Sandalio LM, Leterrier M, Rodríguez-Serrano MM, Del Río LA, Palma JM (2006) Glutathione reductase from pea leaves: response to abiotic stress and characterization of the peroxisomal isozyme. New Phytol **170:** 43–52

Romero-Puertas MC, Ortega-Galisteo A, Rodríguez-Serrano M, Sandalio LM (2012) Insights into cadmium toxicity: reactive oxygen and nitrogen species function. *In* **Gupta DK, Sandalio LM**, eds, Metal Toxicity in Plants: Perception, Signaling and Remediation. Springer, Berlin, pp 91–117

Romero-Puertas MC, Palma JM, Gomez M, Del Río LA, Sandalio LM (2002) Cadmium causes the oxidative modification of proteins in pea plants. Plant Cell Environ **25:** 677–686

Romero-Puertas MC, Rodríguez-Serrano M, Corpas FJ, Gomez M, Del Río LA, Sandalio LM (2004) Cadmium-induced subcellular accumulation of $O_2^{\bullet-}$ and H_2O_2 in pea leaves. Plant Cell Environ **27:** 1122–1134

Sandalio LM, Dalurzo HC, Gómez M, Romero-Puertas MC, del Río LA (2001) Cadmium-induced changes in the growth and oxidative metabolism of pea plants. J Exp Bot **52:** 2115–2126

Sandalio LM, Rodríguez-Serrano M, Gupta D, Archilla A, Romero-Puertas MC, Del Río LA (2012) Reactive oxygen species and nitric oxide in plants under cadmium stress: from toxicity to signaling. *In* **Ahmad P, Prasad MNV**, eds, Environmental Adaptations and Stress Tolerance of Plants in the Era of Climate Change. Springer, New York, pp 199–215

Schützendubel A, Nikolova P, Rudolf C, Polle A (2002) Cadmium and H_2O_2-induced oxidative stress in *Populus* × *canescens* roots. Plant Physiol Biochem **40:** 577–584

Schützendübel A, Polle A (2002) Plant responses to abiotic stresses: heavy metal-induced oxidative stress and protection by mycorrhization. J Exp Bot **53:** 1351–1365

Schützendübel A, Schwanz P, Teichmann T, Gross K, Langenfeld-Heyser R, Godbold DL, Polle A (2001) Cadmium-induced changes in antioxidative systems, hydrogen peroxide content, and differentiation in Scots pine roots. Plant Physiol **127:** 887–898

Seth CS, Remans T, Keunen E, Jozefczak M, Gielen H, Opdenakker K, Weyens N, Vangronsveld J, Cuypers A (2012) Phytoextraction of toxic metals: a central role for glutathione. Plant Cell Environ **35:** 334–346

Shannon P, Markiel A, Ozier O, Baliga NS, Wang JT, Ramage D, Amin N, Schwikowski B, Ideker T (2003) Cytoscape: a software environment for integrated models of biomolecular interaction networks. Genome Res **13:** 2498–2504

Sharma SS, Dietz KJ (2009) The relationship between metal toxicity and cellular redox imbalance. Trends Plant Sci **14:** 43–50

Solti A, Gáspár L, Mészáros I, Szigeti Z, Lévai L, Sárvári E (2008) Impact of iron supply on the kinetics of recovery of photosynthesis in Cd-stressed poplar (*Populus glauca*). Ann Bot (Lond) **102:** 771–782

Tamás L, Dudíková J, Durceková K, Halusková L, Huttová J, Mistrík I, Ollé M (2008) Alterations of the gene expression, lipid peroxidation, proline and thiol content along the barley root exposed to cadmium. J Plant Physiol **165:** 1193–1203

Tamoi M, Tabuchi T, Demuratani M, Otori K, Tanabe N, Maruta T, Shigeoka S (2010) Point mutation of a plastidic invertase inhibits development of the photosynthetic apparatus and enhances nitrate assimilation in sugar-treated Arabidopsis seedlings. J Biol Chem **285:** 15399–15407

Thimm O, Bläsing O, Gibon Y, Nagel A, Meyer S, Krüger P, Selbig J, Müller LA, Rhee SY, Stitt M (2004) MAPMAN: a user-driven tool to display genomics data sets onto diagrams of metabolic pathways and other biological processes. Plant J **37:** 914–939

Thomine S, Wang RC, Ward JM, Crawford NM, Schroeder JI (2000) Cadmium and iron transport by members of a plant metal transporter family in Arabidopsis with homology to Nramp genes. Proc Natl Acad Sci USA **97:** 4991–4996

Ueno D, Iwashita T, Zhao FJ, Ma JF (2008) Characterization of Cd translocation and identification of the Cd form in xylem sap of the Cd-hyperaccumulator *Arabidopsis halleri*. Plant Cell Physiol **49:** 540–548

Van Belleghem F, Cuypers A, Semane B, Smeets K, Vangronsveld J, d'Haen J, Valcke R (2007) Subcellular localization of cadmium in roots and leaves of *Arabidopsis thaliana*. New Phytol **173:** 495–508

Vazquez MD, Barcelo J, Poschenrieder C, Madico J, Hatton P, Baker AJM, Cope GH (1992) Localization of zinc and cadmium in *Thlaspi Caerulescens* (Brassicaceae), a metallophyte that can hyperaccumulate both metals. J Plant Physiol **140:** 350–355

Verrier PJ, Bird D, Burla B, Dassa E, Forestier C, Geisler M, Klein M, Kolukisaoglu U, Lee Y, Martinoia E, et al (2008) Plant ABC proteins—a unified nomenclature and updated inventory. Trends Plant Sci **13:** 151–159

Vogel-Mikus K, Arcon I, Kodre A (2010) Complexation of cadmium in seeds and vegetative tissues of the cadmium hyperaccumulator *Thlaspi praecox* as studied by X-ray absorption spectroscopy. Plant Soil **331:** 439–451

Vollenweider P, Cosio C, Gunthardt-Goerg MS, Keller C (2006) Localization and effects of cadmium in leaves of a cadmium-tolerant willow (*Salix viminalis* L.): Part II. Microlocalization and cellular effects of cadmium. Environ Exp Bot **58:** 25–40

Weber M, Trampczynska A, Clemens S (2006) Comparative transcriptome analysis of toxic metal responses in *Arabidopsis thaliana* and the $Cd^{(2+)}$-hypertolerant facultative metallophyte *Arabidopsis halleri*. Plant Cell Environ **29:** 950–963

Wei HR, Persson S, Mehta T, Srinivasasainagendra V, Chen L, Page GP, Somerville C, Loraine A (2006) Transcriptional coordination of the metabolic network in Arabidopsis. Plant Physiol **142:** 762–774

Wintz H, Vulpe C (2002) Plant copper chaperones. Biochem Soc Trans **30:** 732–735

Wójcik M, Tukiendorf A (2004) Phytochelatin synthesis and cadmium localization in wild type of *Arabidopsis thaliana*. Plant Growth Regul **44:** 71–80

Wu HL, Chen CL, Du J, Liu H, Cui Y, Zhang Y, He YJ, Wang YQ, Chu CC, Feng ZY, et al (2012) Co-overexpression *FIT* with *AtbHLH38* or *AtbHLH39* in Arabidopsis-enhanced cadmium tolerance via increased cadmium sequestration in roots and improved iron homeostasis of shoots. Plant Physiol **158:** 790–800

Xu J, Sun J, Du L, Liu X (2012) Comparative transcriptome analysis of cadmium responses in *Solanum nigrum* and *Solanum torvum*. New Phytol **196:** 110–124

Yamaguchi H, Fukuoka H, Arao T, Ohyama A, Nunome T, Miyatake K, Negoro S (2010) Gene expression analysis in cadmium-stressed roots of a low cadmium-accumulating solanaceous plant, *Solanum torvum*. J Exp Bot **61:** 423–437

Yi XP, Hargett SR, Frankel LK, Bricker TM (2009) The PsbP protein, but not the PsbQ protein, is required for normal thylakoid architecture in *Arabidopsis thaliana*. FEBS Lett **583:** 2142–2147

Zhang LD, Yu SW, Zuo KJ, Luo LJ, Tang KX (2012) Identification of gene modules associated with drought response in rice by network-based analysis. PLoS ONE **7:** e33748

Zuther E, Büchel K, Hundertmark M, Stitt M, Hincha DK, Heyer AG (2004) The role of raffinose in the cold acclimation response of *Arabidopsis thaliana*. FEBS Lett **576:** 169–173